Turning Noise into Numbers: Simultaneous estimation of the radioactivity distribution and electron density map from scattered coincidences in PET

Hongyan Sun[1,2], Geng Zhang[1,2], Stephen Pistorius[1,2,3]

[1] Physics and Astronomy, University of Manitoba, Winnipeg, Canada
[2]CancerCare Manitoba, Winnipeg, Canada
[3]Radiology, University of Manitoba, Winnipeg, Canada

Abstract— **Scattered coincidences are typically considered as noise which degrades image contrast and compromises quantitative accuracy in positron emission tomography (PET). Additionally, an anatomical image is required to provide accurate attenuation correction and to facilitate the interpretation of the activity distribution. By accurately measuring the scattered photon energies and taking advantage of the kinematics of Compton scattering, two circular arcs (TCA) can be identified for each scattered coincidence which describes the possible scattering loci and encompasses the annihilation position. Using this premise, we have developed novel iterative reconstruction algorithms which use scattered coincidences to 1) improve the activity distribution and 2) obtain an electron density map. The results have demonstrated the feasibility and benefits of incorporating scattered coincidences into the image reconstruction process. Incorporating scattered coincidences directly into the radiotracer reconstruction algorithm eliminates the need for scatter correction, and can improve both image quality and system sensitivity. The electron density map reconstructed from scattered coincidences can be directly applied to attenuation correction of the activity distribution, which removes energy scaling and registration problems. This work can directly benefit patients by reducing the scanning time and injected radiation dose for equivalent image quality, or improvement in image quality if acquisition time and radiotracer injection are held constant.**

Keywords— **PET, activity distribution, electron density map, scattered coincidences**

I. Introduction

Positron emission tomography (PET) is a powerful metabolic imaging modality based on simultaneously detecting two antiparallel annihilation photons. However, it is possible that one or both photons undergoes Compton scattering prior to detection. The scatter fraction can be as high as 40-60% when the scanner operates in 3D mode or in large patients [1, 2]. Scattered coincidences degrade PET image contrast and compromise quantitative accuracy. Consequently, various scatter correction approaches have been proposed [3, 4]. Most of them estimate and subtract a scatter sinogram from the measured data in pre-correction methods, or by incorporating a constant additive term into the reconstruction algorithm. Inaccuracy in the estimation of the scatter sinogram will introduce significant bias in the estimated activity distribution, while the subtraction based correction methods destroy the Poisson nature of the data, reduce the system's sensitivity, and amplify image noise [5]. Scattered photons also lead to the amount of radiopharmaceuticals injected into patients increased to keep a reasonable contrast to noise ratio in PET images.

The limited spatial resolution (~6-8 mm) of PET images, as well as a lack of anatomical context, makes attenuation correction and the interpretation of the precise location of the radiotracer difficult. Attenuation correction may be carried out using simplistic and often inaccurate approaches or by coupling the PET to CT or MR system [6, 7]. Although the combination of PET and CT is used in commercial scanners, PET/CT has several limitations. Its main drawback is that the imaging is performed sequentially rather than simultaneously, which may introduce artifacts when registering the functional and anatomical images. Due to the different energies used in PET and CT, the attenuation map measured at CT energies must be rescaled to the energy of interest for PET. In addition, radiation dose to patients is increased by this process. Combining PET and MRI is challenging, as conventional PET systems use detectors which are sensitive to magnetic fields, and it is difficult to relate MRI images to the coefficients required to correct for attenuation of the PET annihilation photons.

Since the scattered photons also carry some probabilistic information about the spatial distribution of the annihilation positions, the goal of this project is to extract the latent information from scattered coincidences to 1) improve the image quality of the activity distribution; and 2) extract anatomical information.

II. Methods and materials

A. Scatter reconstruction theory

At the energies of interest in nuclear medicine, Compton scattering is the principal photon interaction and single scattering accounts for more than 80% [1] of the total meas-

ured scattered events. This project is developed based on this observation.

Fig.1(a) illustrates a scattered coincidence in a patient. The unscattered photon is detected at A while the other photon undergoes a Compton scattering and is detected at B with energy E'. The scattering angle θ can be related to the scattered photon energy E' by using the Compton equation [1]. Taking advantage of the kinematics of Compton scattering, two circular arcs (TCA) can be identified, which describe the locus of all the possible scattering positions and encompass the annihilation position. In 3D, the source is located in the volume contained by the surface obtained by rotating the TCA around its axis.

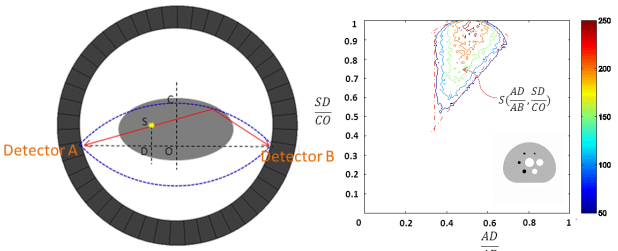

Fig.1(a) A diagram of a Compton scattering event in a patient. The unscattered photon is observed by detector A while the other photon suffers a Compton scattering and is detected at B. This figure also illustrates the two circular arcs (TCA), shown as blue dotted curves, which describe the locus of possible scattering locations and which enclose the annihilation position. (b) The probability map of annihilation positions for NEMA NU2-2001 phantom in normalized coordinates. The distance AB between the two detectors and the distance OC from the center of AB perpendicularly to the TCA have been normalized to unity. Then the annihilation position for a scattered coincidence in the normalized coordinate can be expressed by using the absolute ratio of AD relative to the distance AB as the abscissa and the ratio of SD relative to CO as the ordinate.

The size and shape of the TCA is a function of the scattering angle and the detected photon positions. In the limiting case, where the scattering angle approaches zero, the shape of the TCA approaches the line of response (LOR) for a true coincidence. The true coincidences can be taken as a subset of the scattered coincidences. Thus both true and scattered coincidences can be used to extract the activity distribution in a consistent way. The uncertainty in specifying the TCA is related to the energy resolution of the detectors.

B. Estimating the activity distribution

We have used this knowledge to generalize the Maximum-Likelihood Expectation Maximization (ML-EM) reconstruction algorithm [8, 9] in list-mode to directly incorporate scattered coincidences into the image reconstruction algorithm, instead of correcting for them as in conventional emission imaging methods, as expressed in the following form:

$$\vec{f}_i^{n+1} = f_i^n \frac{1}{\sum_{j'=1}^{N} a_{j',i}} \sum_{j=1}^{N} a_{j,i} \frac{1}{\sum_{i'=1}^{p} a_{j,i'} f_{i'}^n * att} \qquad i = 1, \dots, p \tag{1}$$

where p is the total number of pixels in the image, N is the total number of detected coincidences and $a_{j,i}$ is the element of the system matrix characterizing the probability that the annihilation photons detected as the j^{th} coincidence (whether scattered or not) were emitted from pixel i. *att* is the attenuation correction coefficient for a scattered coincidence, which can be can be estimated by averaging the attenuation coefficient over all possible scattering loci described by the TCA and weighted by the electron density and photon flux at each possible scattering position.

The main difference between this Generalized Scatter ML-EM algorithm (GS-MLEM) and the conventional ML-EM algorithm (LOR-MLEM) is that projection/back-projection process is applied over the area within the TCA or 3D volume instead of along the LOR. Thus, this Generalized Scatter reconstruction method uses both true and scattered coincidences in a consistent way to reconstruct the activity distribution.

To further improve the reconstructed image quality, the different probabilities of annihilation positions within the TCA can be modeled in normalized coordinates as illustrated in Fig 1(b). The distance AB between the two detectors and the distance OC from the center of AB perpendicularly to the TCA have been normalized to unity. Then the annihilation position for a scattered coincidence in the normalized coordinate can be expressed by using the absolute ratio of AD relative to the distance AB as the abscissa and the ratio of SD relative to CO as the ordinate. Instead of projecting/backprojecting uniformly within TCA, this map will assign a larger weight to the area where the source is more likely found. The non-ideal energy resolution of PET scanners only blurs this probability map in the vertical direction. The benefit of introducing the blurred map into the GS reconstruction to deal with the non-ideal energy resolution is also reported in this paper.

C. Extracting the electron density map

The probability of a Compton interaction occurring is linearly proportional to the electron density of the material. The TCA describes all possible scattering positions. Back-projecting the scattered events along the arcs connecting the two detectors will allow a Compton scattering probability map to be calculated. This map is a function of both radioactive source distribution and the electron density of materials. The influence of the varying photon fluence can be modeled by a sensitivity factor which varies for each pixel

in the ML-EM algorithm. The difference between this algorithm, which reconstructs the anatomical information, and the previously described algorithm which enhances the activity distribution, is that the summation for each coincidence is along the arcs in 2D (or surface in 3D) instead of over the area (or volume in 3D) confined by the arcs.

III. Results

A. Reconstruction activity distribution

Fig.2(a) illustrates the image reconstructed from 3×10^5single-scattered coincidences using a conventional PET reconstruction algorithm (LOR-MLEM). As illustrated in Fig.2(a), scattered coincidences only contribute noise to the resultant image in the conventional algorithm. Fig.2(b) and Fig.2(c) show the images reconstructed from the same scattered data using the GS-MLEM algorithm without and with the inclusion of the probability of annihilation positions. The results show that the proposed algorithm is capable of extracting the activity distribution from scattered events. Including the probability map in the reconstruction speeds up convergence and improves image quality.

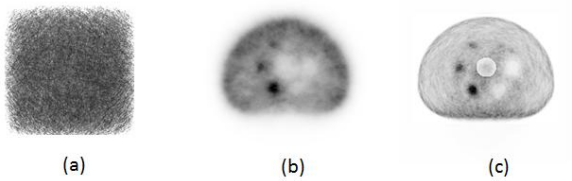

Fig.2(a) Image reconstructed from 3×10^5 scattered coincidences using the conventional LOR-MLEM method. Fig.2(b) and Fig.2(c) are reconstructed from the same scattered coincidences dataset as used in Fig.2(a) by using the GS-MLEM without and with introducing the probability map into the reconstruction.

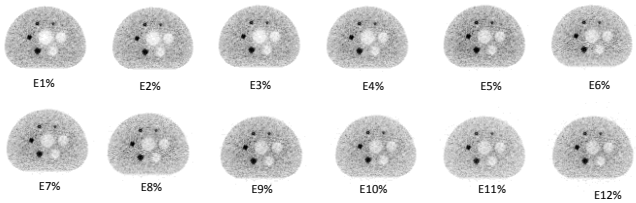

Fig.3 the images reconstructed from the measured data with a scatter fraction of 50% for the energy resolution from 1-12% by using the proposed method.

In practice, both true and scattered coincidences will be incorporated in the PET reconstruction. Fig.3 shows the images reconstructed from measured data with a scatter fraction of 50% and energy resolutions ranging from 1% to 12%. As expected, the GS reconstruction was compromised as the energy resolution became worse. However, the proposed method still achieved better contrast and noise properties up to a 6% energy resolution when compared to the scattered correction based method. At the same time, the sensitivity of the system has improved by 50%.

B. Electron density map reconstruction

Fig.4 shows the electron density map of a ring water phantom reconstructed from scattered coincidences with a single source (Fig.4(d)), two point sources (Fig.4(e)), and a circular uniform source (Fig.4(e)). The results show that it is possible to reconstruct the electron density map from scattered coincidences in PET. For two sources, or a distributed source, the crosstalk between the functional and anatomical content appears as shown Fig.4(e) and (f). However, the crosstalk can be minimized by jointly estimating the electron density and activity distribution from both true and scattered events. Further investigation is underway to reduce this effect.

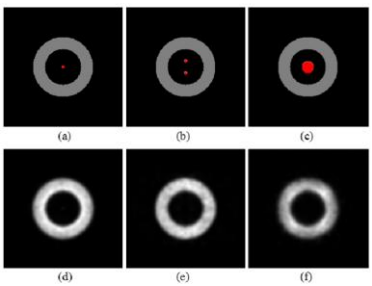

Fig.4 The electron density map of a circular ring uniform water phantom. Upper row shows the phantom with the source distribution displayed in red. The lower rows show the corresponding reconstructions.

IV. CONCLUSIONS

This project has demonstrated the feasibility and benefit of extracting both activity and electron density information from scattered coincidences. Incorporating scattered coincidences directly into the radiotracer reconstruction algorithm eliminates the need for scatter correction, and could improve both image quality and system sensitivity. The electron density map reconstructed from scattered coincidences can be directly applied to attenuation correction for the activity distribution, which will provide for more accurate attenuation correction and interpretation of the metabolic images at a reduced cost. Thus this work finally leads to more accurate diagnosis for patient with reduced radiation dose and make PET more accessible to public.

References

1. D. L. Bailey, D. W. Townsend, P. E. Valk, and M. N. Maisey, Positron Emission Tomography: Basic Sciences,2005.

2. A. Konik, M. T. Madsen, and J. J. Sunderland, "GATE Simulations of Human and Small Animal PET for Determination of Scatter Fraction as a Function of Object Size," IEEE Trans. Nucl. Sci., vol. 57, no. 5, pp. 2558-2563, 2010.
3. H. Zaidi and M.-L. Montandon, "Scatter Compensation Techniques in PET," PET Clin., vol. 2, pp. 219-234, 2007.
4. H. Zaidi and K. F. Koral, "Scatter modelling and compensation in emission tomography," Eur. J. Nucl. Med. Mol. Imaging., vol. 31, pp. 761-782, 2004.
5. L. M. Popescu, "PET Energy-Based Scatter Estimation in the Presence of Randoms, and Image Reconstruction With Energy-Dependent Scatter and Randoms Corrections," IEEE Trans. Nul. Sci., Vol. 59, pp. 1958-1966, 2012.
6. V. Bettinardi, L. Presotto, E. Rapisarda, M. Picchio, L. Gianolli, and M. C. Gilardi, "Physical Performance of the new hybrid PET/CT Discovery-690," Med. Phys., vol. 38, pp. 5394-5411, no.10, 2011.
7. M. S. Judenhofer, et. al, "Simultaneous PET-MRI: a new approach for functional and morphological imaging," Nature Medicine, vol. 14, pp. 459-465, 2008.
8. L. A. Shepp and Y. Vardi, "Maximum Likelihood Reconstruction for Emission Tomography," IEEE Trans. Med. Imaging, vol. MI-1, 1982.
9. C. Byrne, "Likelihood Maximization for List-Mode Emission Tomographic Image Reconstruction," IEEE Trans. Med. Imaging, vol. 20, No.10, pp.1084-1092, 2001.